Original Article

Validation of prognostic signature and exploring the immune-related mechanisms for *NR3C2* in clear cell renal cell carcinoma

Daoxun Chen[1], Zhenjie Yin[1], Yongmei Chen[1], Yuanyuan Bai[1], Bingyong You[1], Yingming Sun[2], Yongyang Wu[1]

[1]Department of Urology, Affiliated Sanming First Hospital, Fujian Medical University, Sanming, China; [2]Department of Medical and Radiation Oncology, Affiliated Sanming First Hospital, Fujian Medical University, Sanming, China

Contributions: (I) Conception and design: Y Wu, Y Sun; (II) Administrative support: Y Wu; (III) Provision of study materials or patients: D Chen, Z Yin; (IV) Collection and assembly of data: Y Chen, B You, Y Bai; (V) Data analysis and interpretation: D Chen; (VI) Manuscript writing: All authors; (VII) Final approval of manuscript: All authors.

Correspondence to: Yongyang Wu, MD, PhD. Department of Urology, Affiliated Sanming First Hospital, Fujian Medical University, No. 29 Liedong Road, Meilie District, Sanming 365000, China. Email: wuyyfj@fjmu.edu.cn.

Background: Previous studies have verified that *NR3C2* inhibits tumor cell proliferation, invasion, and migration. However, there is a lack of independent validation cohorts for verifying the prognostic value of *NR3C2* in clear cell renal cell carcinoma (ccRCC), and its underlying antitumor mechanisms remain unclear.

Methods: We first obtained dates from the online public databases. Then R language or online public database was used for bioinformatics analyses to evaluate the effect of *NR3C2* on the diagnosis, prognosis, and immune microenvironment in ccRCC patients. Finally, the results were verified by our own cohort and immunofluorescence (IF) staining.

Results: The present study yielded significant findings regarding the expression of *NR3C2* in ccRCC compared to control tissues. Specifically, *NR3C2* expression was found to be significantly reduced in ccRCC and was observed to be correlated with tumor stage. Additionally, patients with lower *NR3C2* expression exhibited shorter overall survival (OS), disease-specific survival, and progress-free survival. Univariable and multivariate Cox analyses further identified *NR3C2* expression as an independent prognostic factor for ccRCC. Receiver operating characteristic (ROC) analysis demonstrated that *NR3C2* was a highly accurate marker for distinguishing tumors from normal kidney tissue, with an area under the curve (AUC) of 0.959. Further analyses using Gene Ontology (GO) and Kyoto Encyclopedia of Genes and Genomes (KEGG) pathway analysis suggested that *NR3C2* may play a role in various biological processes and pathways related to tumor immune microenvironment (TIM). The expression of *NR3C2* exhibited significant positive correlations with the levels of infiltration of $CD4^+$ and $CD8^+$ T cells, as well as an association with immune checkpoints.

Conclusions: Our exploratory study suggested that *NR3C2* could serve as a novel biomarker for predicting survival in patients with ccRCC and the molecular mechanisms owe partly to immune cell infiltration.

Keywords: *NR3C2*; clear cell renal cell carcinoma (ccRCC); prognosis; immune; T cells

Submitted May 17, 2023. Accepted for publication Sep 22, 2023. Published online Oct 24, 2023.
doi: 10.21037/tcr-23-846
View this article at: https://dx.doi.org/10.21037/tcr-23-846

Introduction

Renal cell carcinoma (RCC) accounts for roughly 90% of kidney malignancies and 3% of all cancers in human (1). About 85% of RCC are clear cell renal cell carcinoma (ccRCC) (2). Despite the fact that surgery may be curative for early-stage ccRCC, recurrences are common after surgery, and late-stage, inoperable cancer is usually fatal (3). Over the last few decades, immunotherapy has grown in importance and has been acknowledged as a promising therapy for cancer patients (4). In ccRCC, immune checkpoint blockade (ICB) is gaining prominence and is being used in combination with vascular endothelial growth factor (VEGF) tyrosine kinase inhibitors (TKIs) (5). However, the resistance of ICB occurs in most patients (6). There is still a long way to go in developing immunotherapy for ccRCC.

NR3C2 is responsible for encoding the receptor for hormones produced by the adrenal cortex (7). *NR3C2* contains ten exons and is located on chromosome 4q31.23 (8). NR3C2 protein is expressed in a variety of cell types, including those in the gastrointestinal tract, immune cells, the brain, heart, bones, skin, and skeletal muscles (9). Recent studies have demonstrated its inhibitory effects on tumor cell proliferation, invasion, and migration. Moreover, it is noteworthy that *NR3C2* is also associated with immune cell infiltration (10,11). Due to the role of aldosterone in the transepithelial transport of sodium, potassium, and water, early studies of *NR3C2* were conducted by nephrologists. Notably, low *NR3C2* expression has been linked to poor prognosis in non-distant metastatic ccRCC patients (12), although the underlying mechanisms remain elusive. Therefore, it is imperative to conduct an in-depth investigation on this phenomenon.

Based on the above research, we aimed to validate the anti-ccRCC effect of *NR3C2* with dependent cohorts. Notably, we explored the underlying mechanism of *NR3C2* and its relationship with tumor immune microenvironment (TIM) of ccRCC. We present this article in accordance with the TRIPOD reporting checklist (available at https://tcr.amegroups.com/article/view/10.21037/tcr-23-846/rc).

Highlight box

Key findings

- *NR3C2* was validated for its prognostic value in clear cell renal cell carcinoma (ccRCC) and the molecular mechanisms owed partly to immune cell infiltration.

What is known and what is new?

- Low *NR3C2* expression was associated with a poor prognosis in patients with non-distant metastatic ccRCC.
- The molecular mechanisms of *NR3C2* owe partly to immune cell infiltration.

What is the implication, and what should change now?

- More attention should be paid to the relationship between *NR3C2* and tumor immune microenvironment.

Methods

Data extraction from public databases

The Cancer Genome Atlas (TCGA, https://tcga.xenahubs.net), the Gene Expression Omnibus (GEO, http://www.ncbi.nlm.nih.gov/geo/) database (13), and the EMBL-EBI database (https://www.ebi.ac.uk/) were the source of data on the expression of the *NR3C2* gene and clinical information pertaining to ccRCC patients. Pan-cancer analysis was performed with Gene Set Cancer Analysis (GSCA, http://bioinfo.life.hust.edu.cn/GSCA/#/), Gene Expression Profiling Interactive Analysis (GEPIA2, http://gepia2.cancer-pku.cn/#index) database and cBioPortal (http://www.cbioportal.org/). We extracted 72 non-tumor and 539 tumor tissues from TCGA. The *NR3C2* expression data were retrieved from the GSE68417 and GSE53000 datasets in the GEO database to authenticate the *NR3C2* expression level in both tumor and non-tumor tissues. Additionally, the E-MTAB-1980 cohort from the EMBL-EBI database was employed as an independent validation cohort (14).

Tissue microarray

We purchased the ccRCC tissue microarray from Outdo (Shanghai, China), comprising 149 ccRCC tissues and 30 paired paracancer tissues, accompanied by their clinical and survival data, among other details. The samples were sourced from the National Human Genetic Resources Sharing Service (2005DKA21300). Immunofluorescence (IF) was employed to detect all points on the chip, and the expression of *NR3C2*, $CD4^+$ T cells, and $CD8^+$ T cells was gauged by IF intensity and positive count. A total of 149 patients were stratified into two cohorts utilizing the optimal *NR3C2* cut-off value. Subsequently, survival curves were generated to ascertain the prognostic relevance of these groups. Furthermore, an exploration of the association among *NR3C2*, $CD4^+$ T cells and $CD8^+$ T cells was conducted.

IF staining

The tissue microarrays underwent deparaffinization using graded alcohol, followed by three washes with phosphate-buffered saline (PBS). Subsequently, permeabilization was achieved using 0.4% Triton X-100 for a duration of 30 minutes, and blocking was performed using goat serum working liquid (Wuhan Boster Biological Technology, Wuhan, China) for a period of two hours after antigen retrieval. The sections were then subjected to overnight incubation at 4 ℃ with mixed primary antibodies, followed by washing with PBS to eliminate unbound primary antibodies. Finally, the sections were incubated with secondary antibodies in the dark at room temperature (RT) for a duration of one hour. The sections underwent counterstaining with 4', 6 diamidino-2-phenylindole (Sigma-Aldrich, St. Louis, MO, USA) for a duration of five minutes, followed by washing with PBS. The primary antibodies utilized were *NR3C2* (Proteintech, 21854-1-AP), while the fluorophore-conjugated secondary antibodies employed were goat anti-rabbit Alexa Fluor 488 (1:500; Abbkine, Wuhan, China) and goat anti-mouse Alexa Fluor 549 (1:500; Abbkine). The images were captured through confocal laser scanning microscopy (Nikon A1 + R, Tokyo, Japan), and fluorescence intensity was analyzed using ImageJ software.

Prognosis analysis of NR3C2 in ccRCC

Initially, we investigated the correlation between *NR3C2* and clinical presentations in ccRCC. Subsequently, we employed the Kaplan-Meier (KM) survival and receiver operating characteristic (ROC) curves to evaluate the prognostic efficacy of *NR3C2* in ccRCC patients. Furthermore, we conducted univariate and multivariate COX regression analyses to scrutinize the prognostic relevance of *NR3C2* expression and clinical data. Ultimately, we generated a nomogram diagram and calibration curve to explicate the prognostic significance of *NR3C2*.

Functional analysis of NR3C2 in ccRCC

The limma package in the R software was utilized to investigate the differentially expressed genes (DEGs) of *NR3C2*, with a defined threshold of "Adjusted P<0.05 and Log_2(Fold Change) >1 or Log_2(Fold Change) <–1". Subsequently, volcano and heat maps were generated, and Gene Ontology (GO) and Kyoto Encyclopedia of Genes and Genomes (KEGG) analyses were conducted to explore potential molecular processes and biological pathways associated with *NR3C2* in ccRCC. The R package "clusterProfiler" was employed to perform these analyses for all DEGs in *NR3C2*, with statistical significance defined as P values<0.05.

Tumor Immune Estimation Resource (TIMER) database analysis

TIMER is a comprehensive resource for studying the interaction between genes of interest and tumor immune responses across a wide range of cancer types (https://cistrome.shinyapps.io/timer/) (15). Based on the TCGA, the level of immune infiltrate prevalence was determined across the 32 types of cancer.

KM plotter database analysis

The Online KM plotter tool offers the capacity to compare 54,675 genes across 21 cancer types, utilizing databases such as GEO, TCGA, and the European Genome-phenome Archive (https://kmplot.com/analysis/index.php?p=background). By examining the mRNA expression of CD4, CD8, B cell, macrophage, and neutrophil markers in ccRCC tissues, the KM-plotter tool categorized the ccRCC cohort from TCGA into enriched and decreased infiltration of the aforementioned cell types. Furthermore, the tool was employed to investigate the survival time of ccRCC patients based on the five cell types mentioned above.

Statistical analysis

The data were analyzed using R (version 4.2.2), and SPSS 20.0 software. A number of R packages were used in this study, including ggplot2, pheatmap, limma, survival, survminer, timeROC, rms, and ClusterProfiler. Student's *t*-tests were used to assess the significance of differences between groups. Chi-squared test was used for categorical variables, and Wilcoxon test was used for continuous data. KM and logarithmic rank tests were used to calculate survival differences.

Ethical statement

The study was conducted in accordance with the Declaration of Helsinki (as revised in 2013).

Results

Expression levels and genetic alteration variation of NR3C2 across different cancers

The RNA-sequencing expression profiles and the corresponding clinical information of 33 subjects were obtained from the TCGA dataset, data visualizations were created with R package ggplot2. The down-regulation of *NR3C2* was observed in a significant manner across various cancer types, including breast cancer (BRCA), esophageal squamous cancer (CESC), rectum adenocarcinoma (READ), stomach adenocarcinoma (STAD), bladder cancer (BLCA), colorectal adenocarcinoma (COAD), esophageal cancer (ESCA), glioblastoma multiforme (GBM), head and neck cancer (HNSC), kidney renal clear cell carcinoma (KIRC), kidney renal papillary cell carcinoma (KIRP), liver cancer (LIHC), lung cancer (LUAD and LUSC), prostate cancer (PRAD), thyroid cancer (THCA), and uterine corpus endometrial carcinoma (UCEC), when compared to their respective normal tissues (*Figure 1A*). The similar results were found in GSCA (*Figure 1B*) and GEPIA2 database (*Figure 1C*). The mutation status of *NR3C2* in various tumors was investigated using cBioPortal. The results indicated a relatively high frequency of *NR3C2* variation in bladder cancer, pancreatic cancer, melanoma, and colorectal cancer. Conversely, *NR3C2* variation was infrequent in thyroid cancer, medulloblastoma, cervical cancer, acute myeloid leukemia, mature B-Cell neoplasms, essential thrombocythemia, myelodysplastic/myeloproliferative neoplasms, soft tissue sarcoma, lung cancer, and endometrial cancer (*Figure 1D*). In addition, the heterozygous copy number variation (CNV) (deletion) status of *NR3C2* showed a high proportion in almost all cancers. These findings suggested that *NR3C2* may play a crucial biological role in tumor progression, and genetic changes could influence abnormal *NR3C2* expression in some cancers (*Figure 1E*).

The levels of NR3C2 mRNA and protein in ccRCC

Figure 2A-2D shows the expression of *NR3C2* mRNA in ccRCC from TCGA and GEO. Expression of *NR3C2* in tumor tissue was significantly lower than that in the normal tissue (P<0.001). Immunohistochemical staining images were obtained from the Human Protein Atlas (HPA) database (https://www.proteinatlas.org/) and IF Staining images were used to assess NR3C2 protein expression (*Figure 2E-2H*). The analysis revealed a significant decrease in the protein expression of NR3C2 in tumor tissue compared to normal tissue. To further investigate this phenomenon, IF signal intensity quantification was performed on 30 ccRCC tissues and their adjacent non-cancerous tissues(*Figure 2I*). The results indicated that the median positive expression rate of NR3C2 was higher in normal kidney tissues (43.50%) than in tumor tissues (14.98%).

Prognostic potential of NR3C2

Initially, we investigated the correlation between *NR3C2* and clinical manifestations in ccRCC. The prognostic signature's expression heatmap demonstrated that *NR3C2* expression was significantly associated with T stages, N stages, M stages, stages, and grade stages (P<0.05), while no significant correlation was observed with age or gender (*Figure 3A*). Box plots further revealed that reduced *NR3C2* expression was significantly linked to higher T, N, and M stages, pathological stage, and grade stages (*Figure 3B-3F*). And a greater *NR3C2* expression among female patients as compared to male patients (*Figure 3G*).

Then we explored the association of *NR3C2* with survival outcomes in ccRCC. The association between *NR3C2* expression and survival outcomes was evaluated using the KM survival curve, with the median serving as the threshold for high and low *NR3C2* expression groups. Our findings indicated that patients with elevated *NR3C2* expression exhibited longer overall survival (OS), disease-specific survival, and progress-free interval (P<0.05) (*Figure 4A-4C*). The ROC curve results were reported as AUC scores (*Figure 4D*). The AUC in this trial was 0.959 (95% confidence interval: 0.940–0.978). A validation dataset was acquired from an external source, namely the E-MTAB-1980 cohort. The survival analysis conducted on this cohort revealed that the high-expression group exhibited a favorable prognosis, as depicted in *Figure 4E*. However, the observed difference did not attain statistical significance (P=0.103). In contrast, the survival analysis performed on the cohort tissue microarray cohort demonstrated that the high-expression group had a positive prognosis, as illustrated in *Figure 4F*, and the difference was statistically significant (P<0.05). The characteristics of subjects baseline of tissue microarray are listed in *Table 1*.

Finally, *NR3C2* and clinical data were analyzed in both univariate and multivariate Cox regressions (*Figure 5A,5B*) and the prognostic nomogram and calibration curve of ccRCC were constructed (*Figure 5C,5D*). The univariate Cox model revealed a significant association between a low *NR3C2* level (P<0.001) and OS occurrences in relation

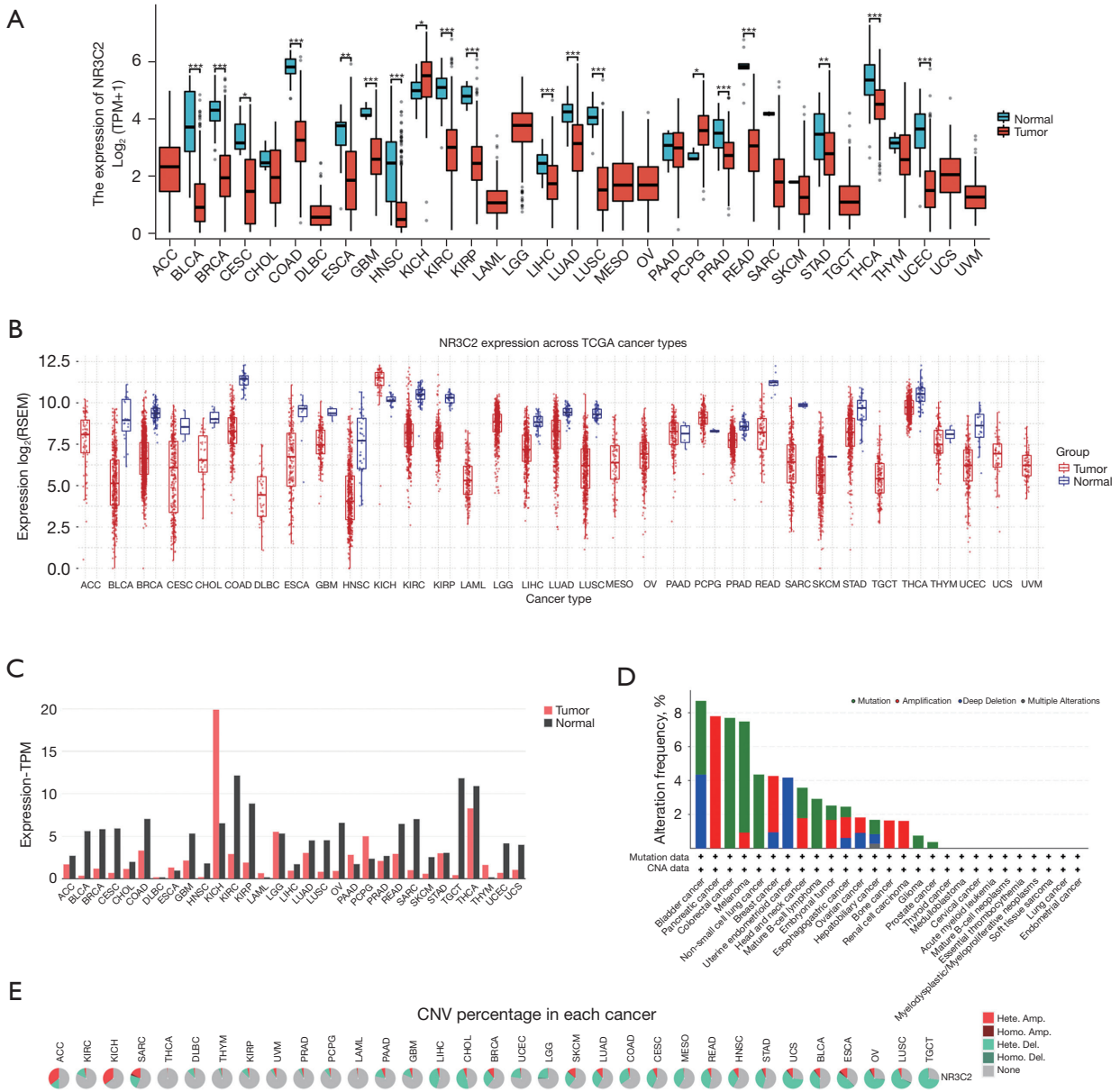

Figure 1 Expression levels and genetic alteration variation of *NR3C2* across different cancers. (A) TCGA datasets indicate that the expression levels of *NR3C2* varied in pan-cancer tissues compared to normal tissues. High or low expression of *NR3C2* in different human cancer tissues compared with normal tissues using the GSCA datasets (B) and GEPIA2 datasets (C), respectively. (D) cBioPortal analysis of *NR3C2* mutations, amplifications, and deletions in different tumors of TCGA. (E) Utilizing the GSCA platform to assess alterations in CNV of *NR3C2* in cancer. *, P<0.05; **, P<0.01; ***, P<0.001. TCGA, The Cancer Genome Atlas; TPM, transcripts per million; GSCA, Gene Set Cancer Analysis; GEPIA2, Gene Expression Profiling Interactive Analysis; CNV, copy number variation.

to age and pathologic TNM stage (P<0.01) in ccRCC. Furthermore, the multivariate Cox model demonstrated that *NR3C2* level, age, and TNM stage were independent variables that were significantly associated with OS in ccRCC (P<0.01).

Exploration of molecular mechanism of NR3C2

On the volcano map, 261 upregulated genes and 33 downregulated genes were distributed among patients with different *NR3C2* expression levels (*Figure 6A*). The

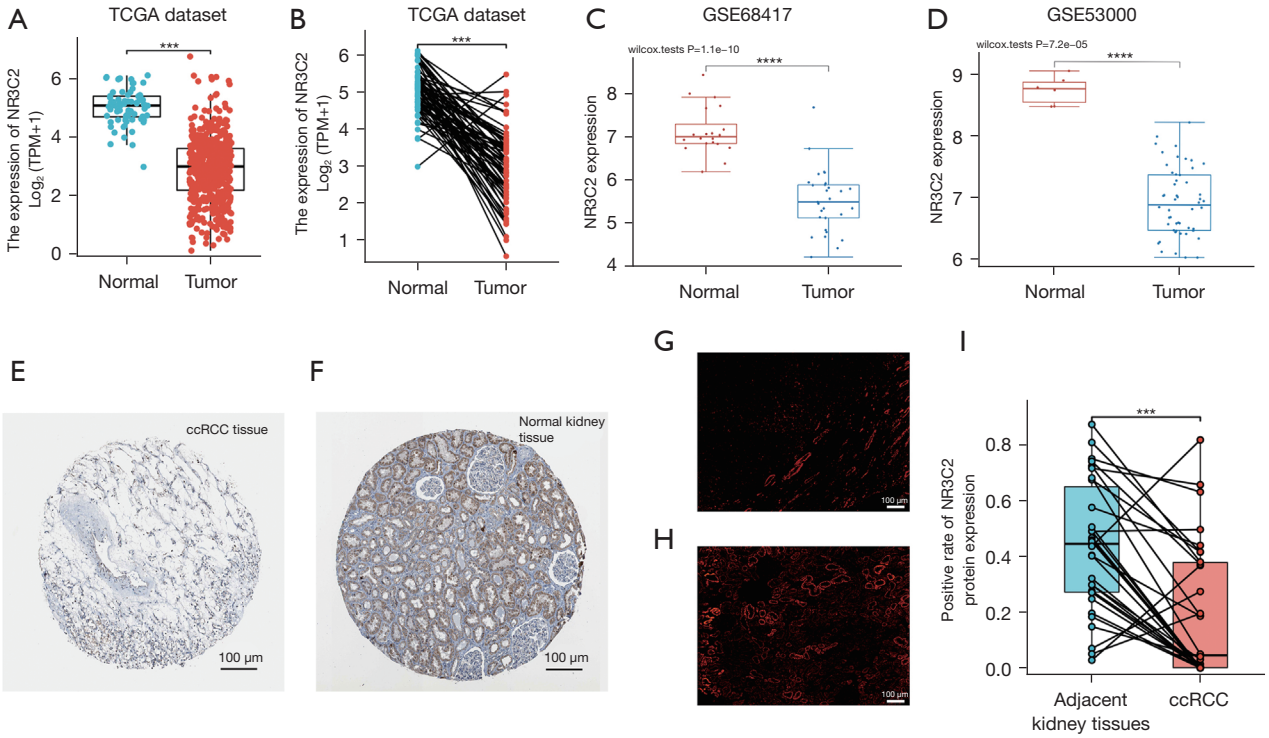

Figure 2 The levels of *NR3C2* mRNA and protein in ccRCC. (A,B) Unpaired and paired samples in TCGA datasets. The expression of *NR3C2* from GSE68417 (C) and GSE53000 (D) in GEO datasets. The level of NR3C2 protein in ccRCC (E) and normal tissues (F) (immunohistochemical staining) obtained from HPA datasets (https://www.proteinatlas.org/). The images of IF staining in ccRCC (G) and normal tissues (H). (I) Protein expression positive rate of NR3C2 in ccRCC and adjacent kidney tissues in tissues microarray. ***, P<0.001; ****, P<0.001. TPM, transcripts per million; ccRCC, clear cell renal cell carcinoma; TCGA, The Cancer Genome Atlas; GEO, Gene Expression Omnibus; HPA, Human Protein Atlas.

expression trend of 50 genes with the highest and lowest differential expression was analyzed on the heat map (*Figure 6B*). Subsequently, KEGG enrichment analysis revealed that the DEGs were predominantly associated with MAPK signaling pathway, PI3K-Akt signaling pathway, Phospholipase D signaling pathway, and Longevity regulating pathway (*Figure 6C*). According to the GO enrichment analysis, biological function of DEGs was mainly focused on kidney development, epithelium migration, epithelial cell migration, cell-substrate adhesion, carboxylic acid transport, and ameboidal-type acid transport (*Figure 6D*). These findings suggested that *NR3C2* primarily impacts cell migration in ccRCC and may regulate the antitumor immune response via the MAPK signaling pathway and other critical immune-related pathways.

The association between NR3C2 and immune cell infiltration in ccRCC

To enhance comprehension of the impact of the *NR3C2* gene on tumor progression, the TIMER database was utilized to investigate the correlation between *NR3C2* expression and tumor-infiltrating immune cells (TIICs) in ccRCC. Interestingly, the result showed that the expression of *NR3C2* was positively correlated with the major immune cell infiltrates, such as $CD4^+$ T cells, $CD8^+$ T cells, macrophages, and neutrophils (*Figure 7A*). *NR3C2* CNV was correlated with the infiltration levels of $CD4^+$ T cells, $CD8^+$ T cells, macrophages and neutrophils (*Figure 7B*). Subsequently, the KM plotter was employed to scrutinize the prognostic implications of *NR3C2* expression in the immune cell subgroup, with the aim of determining whether

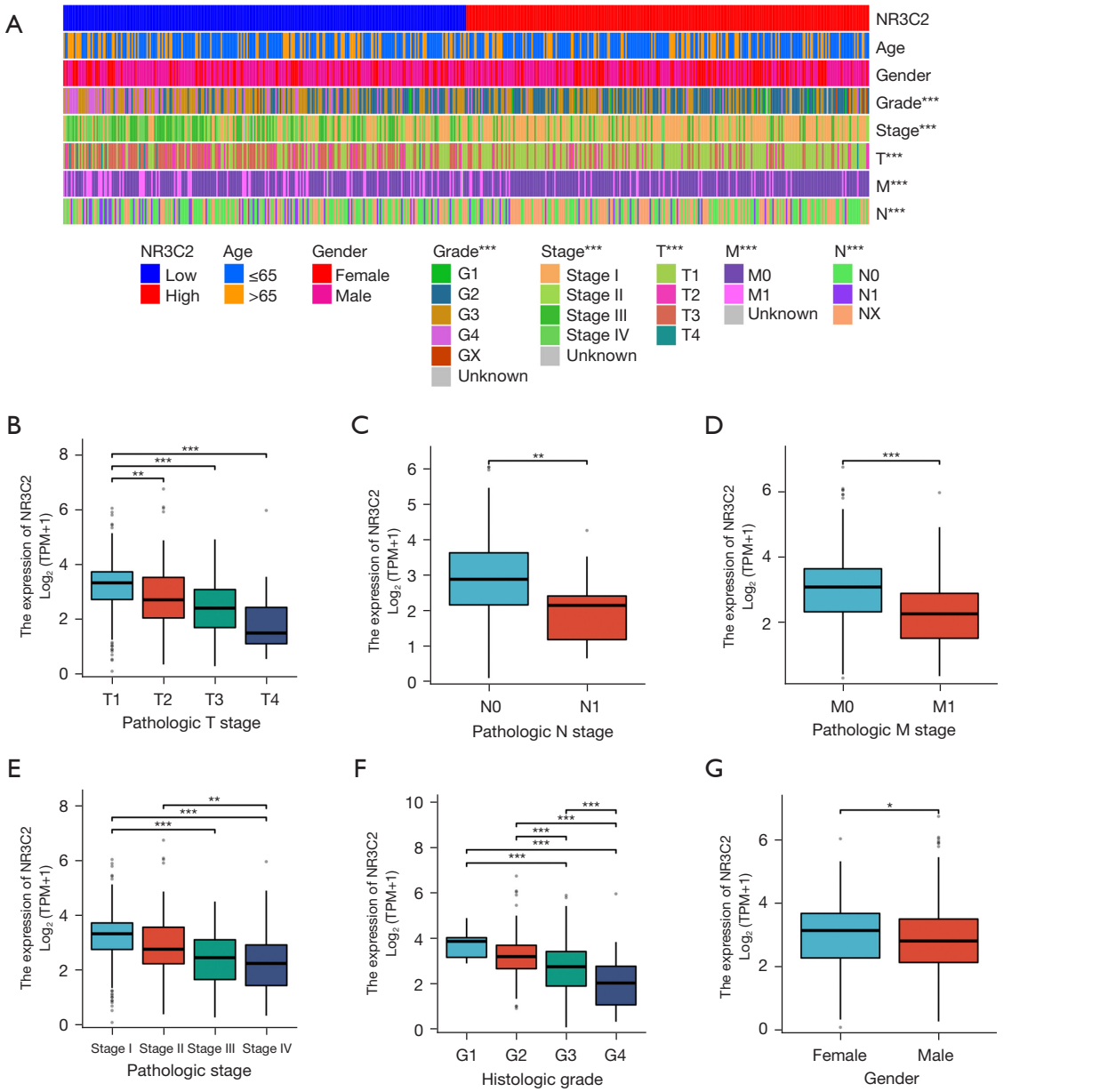

Figure 3 The relationship between *NR3C2* expression and clinical signatures. (A) The expression heatmap of the prognostic signature. (B-D) The correlation between *NR3C2* expression and clinical characteristics, including T, N, and M stages. (E,F) The relationship between *NR3C2* expression and clinical characteristics, including pathologic stages and histological grade. (G) Association between *NR3C2* expression and gender. *, P<0.05; **, P<0.01; ***, P<0.001. TPM, transcripts per million.

the favorable prognosis of ccRCC patients with high *NR3C2* expression is attributable to immune infiltration. The findings indicated that the overexpression of *NR3C2* in ccRCC specimens with either reduced or increased levels of TIICs, including $CD4^+$ T cells, $CD8^+$ T cells, B cells, macrophages, and natural killer (NK) cells, is a significant predictor of a favorable prognosis (*Figure 7C-7G*). Additionally, we employed tissue microarrays as a means of substantiating the aforementioned findings. Specifically, we conducted IF staining on ccRCC tissue microarrays, as depicted in *Figure 7H*. Similar to TIMER database, Our results indicated a noteworthy positive correlation between

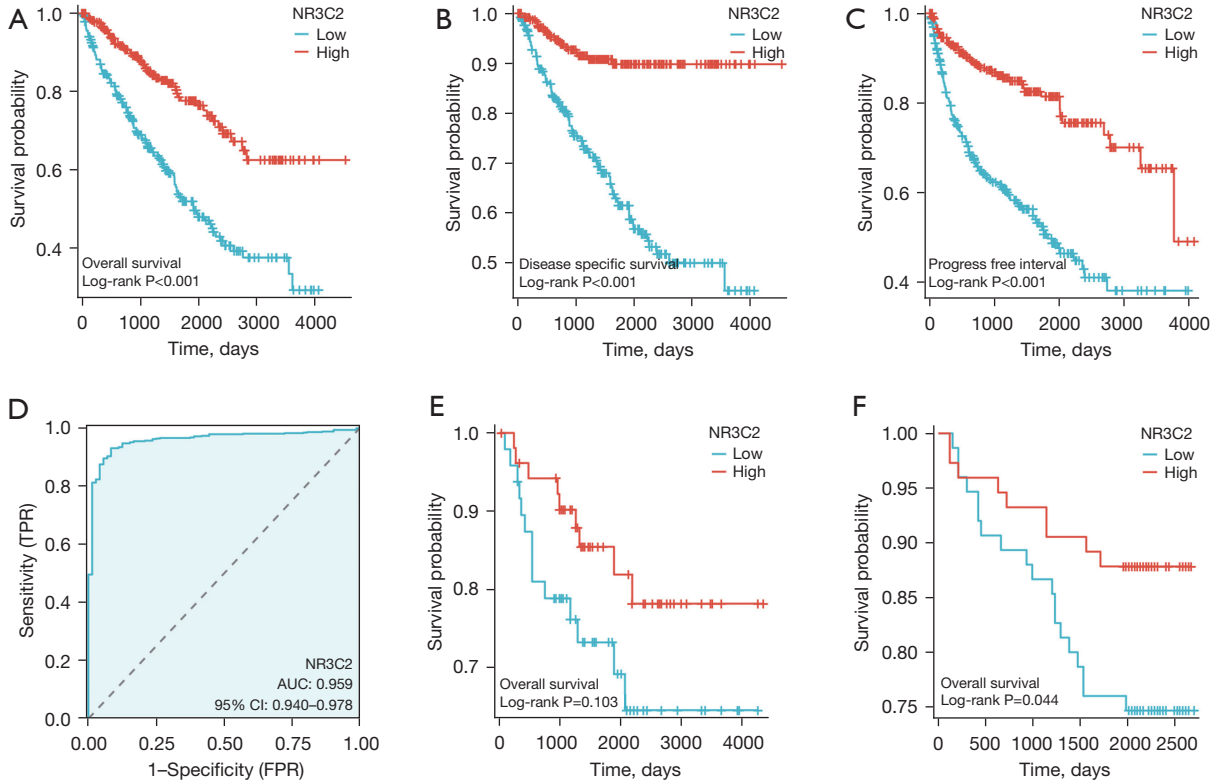

Figure 4 The *NR3C2* prognostic signature in different cohorts. (A-C) The KM survival curve with different *NR3C2* expression in TCGA database. (D) ROC analysis of *NR3C2* in ccRCC patients. (E) Survival curve of patients with different *NR3C2* expression in E-MTAB-1980 cohort. (F) The survival curve of patients exhibiting varying levels of *NR3C2* expression in a tissue microarray. KM, Kaplan-Meier; TCGA, The Cancer Genome Atlas; ROC, receiver operating characteristic; AUC, area under the curve; CI, confidence interval; ccRCC, clear cell renal cell carcinoma; TPR, true positive rate; FPR, false positive rate.

Table 1 *NR3C2* expression and demographic and clinicopathological characteristics

Description	*NR3C2*		N	P value
	Low	High		
Age (years)				0.020
≤65	52	62	114	
>65	23	12	35	
Gender				0.678
Male	55	52	107	
Female	20	22	42	
T				0.030
T1–2	66	72	138	
T3	9	2	11	
N				0.082
N0	72	74	146	
N1–2	3	0	3	

CD4$^+$ T cells and CD8$^+$ T cells with *NR3C2* (*Figure 7I,7J*). Therefore, we concluded that the anti-ccRCC activities of *NR3C2* overexpression may be correlated with high immune cell infiltration.

The association between NR3C2 and immunosuppressive microenvironment in ccRCC

The tumor microenvironment is characterized by a wide spectrum of suppressive signals that shape the (dys-) functional states of intratumoral T cells (16). Therefore, to explore the possible reasons of high T cell infiltration for *NR3C2* overexpression, the transcripts SIGLEC15, TIGIT, CD274, HAVCR2, PDCD1, CTLA4, LAG3, and PDCD1LG2 were identified as relevant to immune checkpoint regulation, and their corresponding expression values were extracted. The box plot showed CTLA4, LAG3, PDCD1, PDCD1LG2, TIGIT were downregulated in patients with high expression *NR3C2*, while CD274,

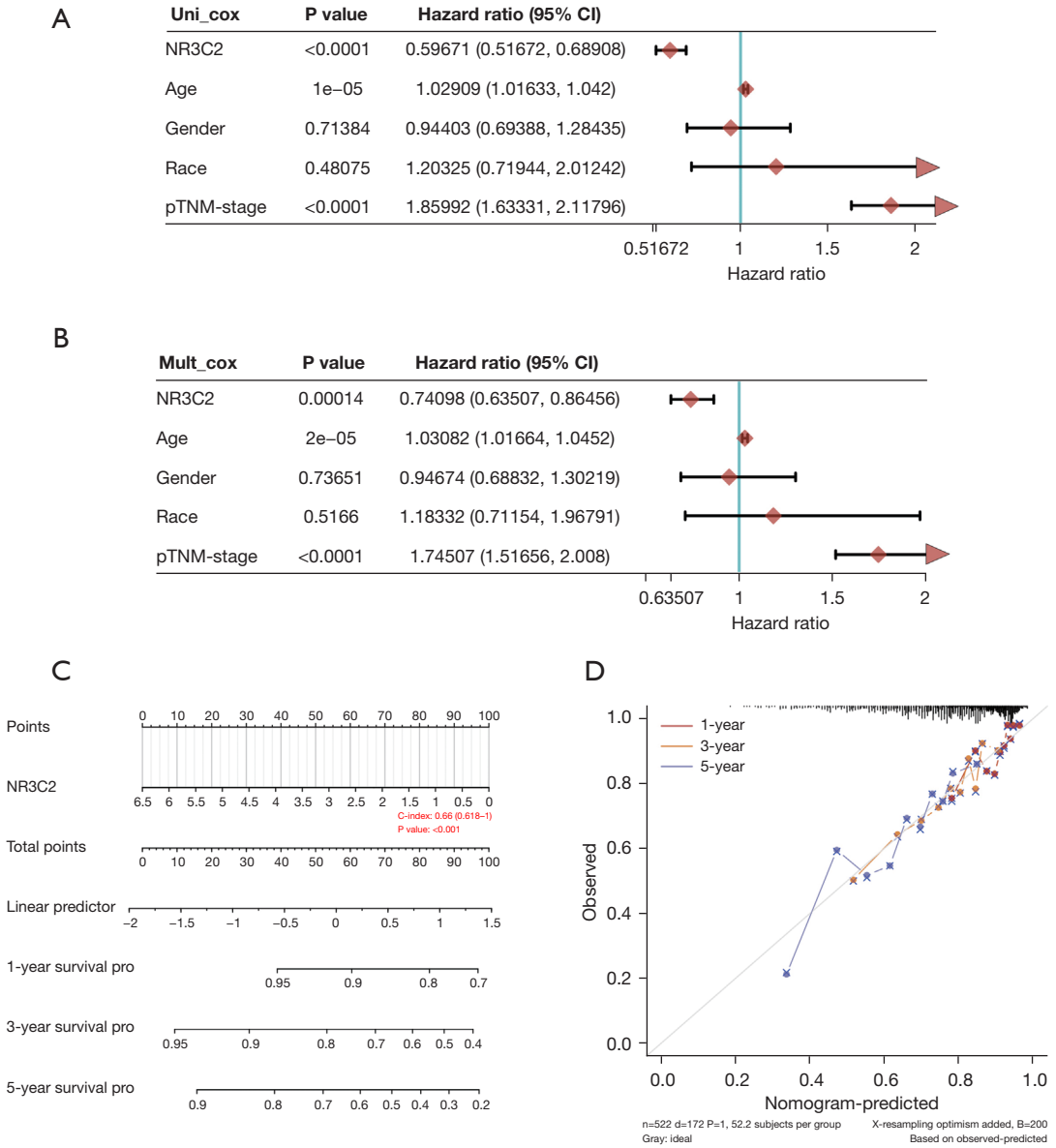

Figure 5 Evaluation of prognostic accuracy of the risk model and other clinicopathological characteristics. (A) The forest plot depicts the results of univariate regression analysis. (B) The forest plot illustrates the outcomes of multivariate regression analysis. *NR3C2*-related nomogram (C) and calibration curve (D). CI, confidence interval; TNM, tumor, node, metastasis.

SIGLEC15 were upregulated (*Figure 8A*). Then, TIMER was used to investigate the correlation between *NR3C2* expression and immunosuppressive molecules, the immune checkpoints. The findings of the analysis indicated a negative correlation between the expression of *NR3C2* and immunosuppressive molecules (PDCD1, CTLA4), immune marker set of myeloid-derived suppressor cell (FUT4), immune marker set of tumor-associated macrophage (CD68), and immune marker sets of regulatory T cell (FOXP3, CCR8) (*Figure 8B*). Finally, we conclude that *NR3C2* may be an adjustable inhibitory immune checkpoint molecule.

Discussion

The current investigation validated the prognostic signature

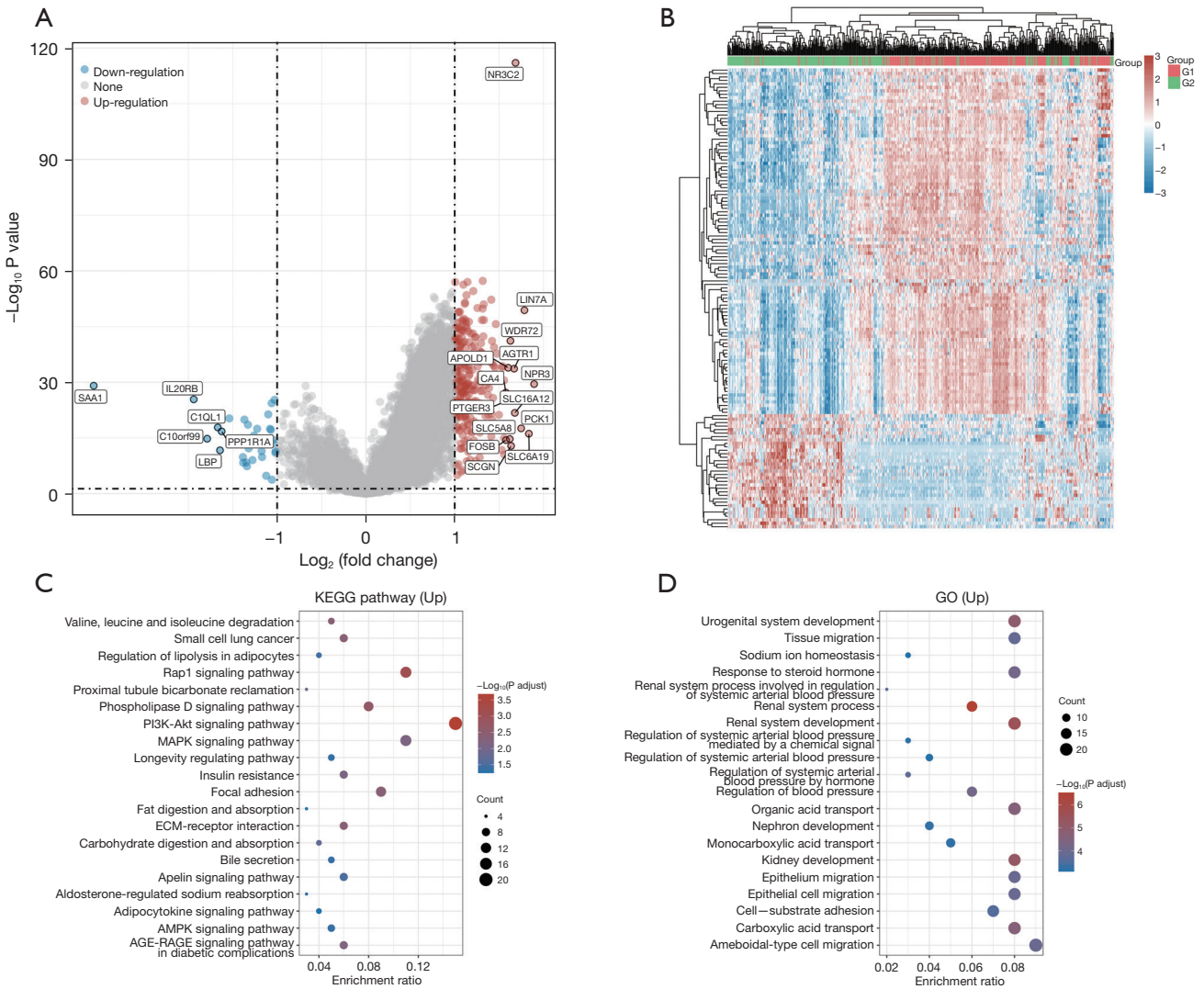

Figure 6 Exploration of molecular mechanism of *NR3C2*. (A) The distribution of DGEs with different levels of *NR3C2* expression. (B) The heat map illustrating the DGEs within high and low expression groups for *NR3C2*. KEGG (C) and GO (D) enrichment analysis of DGEs in *NR3C2* high and low expression groups. DEGs, differentially expressed genes; KEGG, Kyoto Encyclopedia of Genes and Genomes; GO, Gene Ontology.

of *NR3C2* in ccRCC through the utilization of a multi-group independent cohort. Specifically, the expression of *NR3C2* was observed to be diminished in ccRCC tissues in comparison to normal renal tissues, and this was found to be associated with the progression of ccRCC. Patients with lower levels of *NR3C2* expression exhibited shorter OS, disease-specific survival, and progress-free interval. Through the application of univariable Cox analysis, high *NR3C2* expression was identified as an independent prognostic factor for ccRCC, and a prognostic nomogram and calibration curve for ccRCC were constructed. Notably, in the present study, we are the first to demonstrate that *NR3C2* is an accurate marker for identifying tumors from normal kidney tissue based on ROC analysis, and the AUC of the curve was 0.959. To further exploit the anti-tumor mechanism of *NR3C2*, we conducted a GO and KEGG analysis and discovered that the differential genes of *NR3C2* were enriched in various immune-related pathways. Subsequently, we employed IF staining to assess the infiltration of immune cells in ccRCC with varying

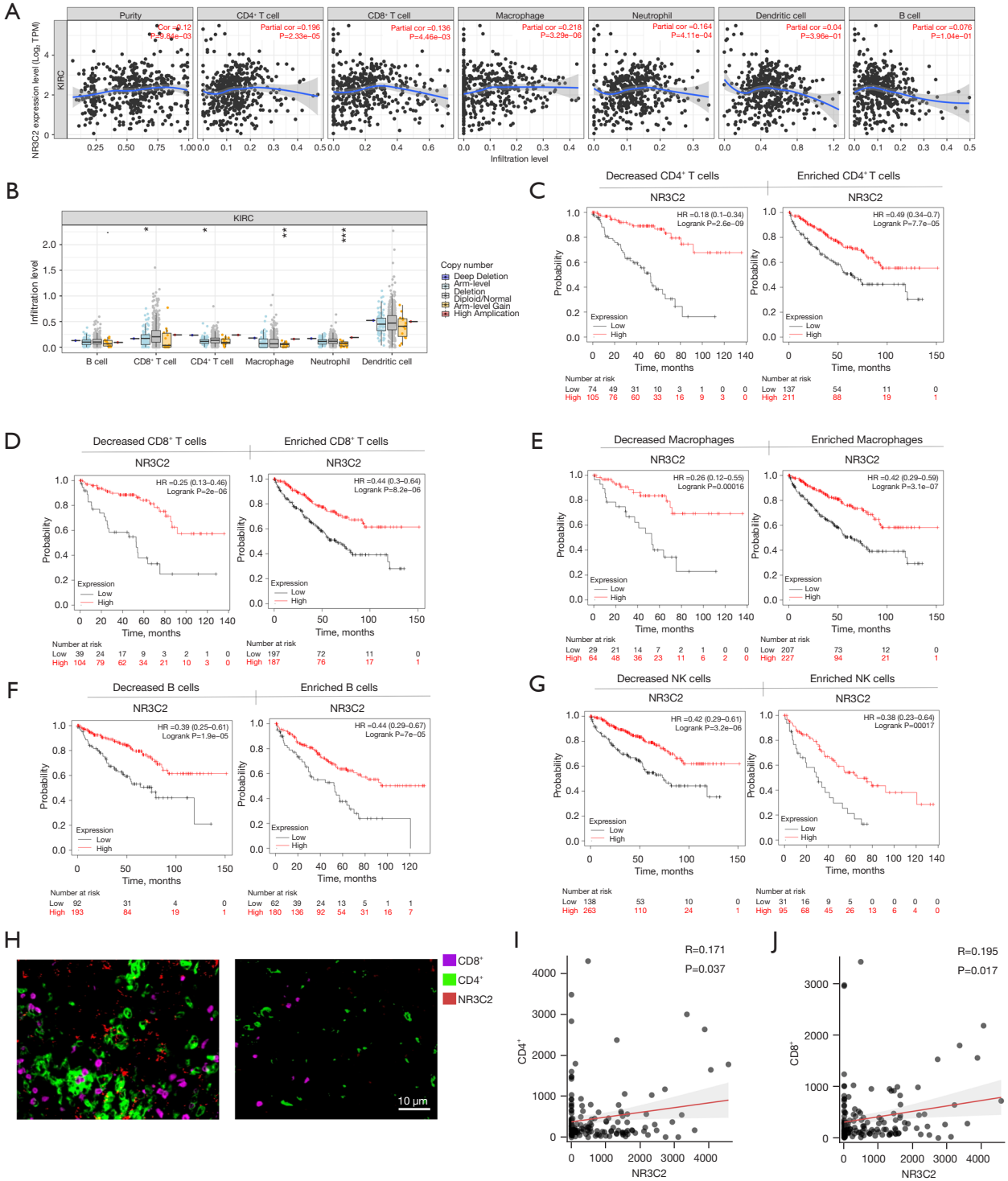

Figure 7 The association between *NR3C2* and immune cell infiltration in ccRCC. (A) An analysis of the TIMER database shows a correlation between tumor purity and *NR3C2* expression. (B) Infiltration levels of immune cells in ccRCC as a result of *NR3C2* CNV. (C-G) Kaplan-Meier overall survival curve of high and low *NR3C2* expression in ccRCC based on the number of tumor-infiltrating immune cells. (H) IF staining in ccRCC tissue microarray. (I) The correlation of *NR3C2* expression with CD4$^+$ T cell. (J) The correlation of *NR3C2* expression with CD8$^+$ T cells. *, P<0.05; **, P<0.01; ***, P<0.001. ccRCC, clear cell renal cell carcinoma; TIMER, Tumor Immune Estimation Resource; CNV, copy number variation; HR, hazard ratio; IF, immunofluorescence; NK, natural killer.

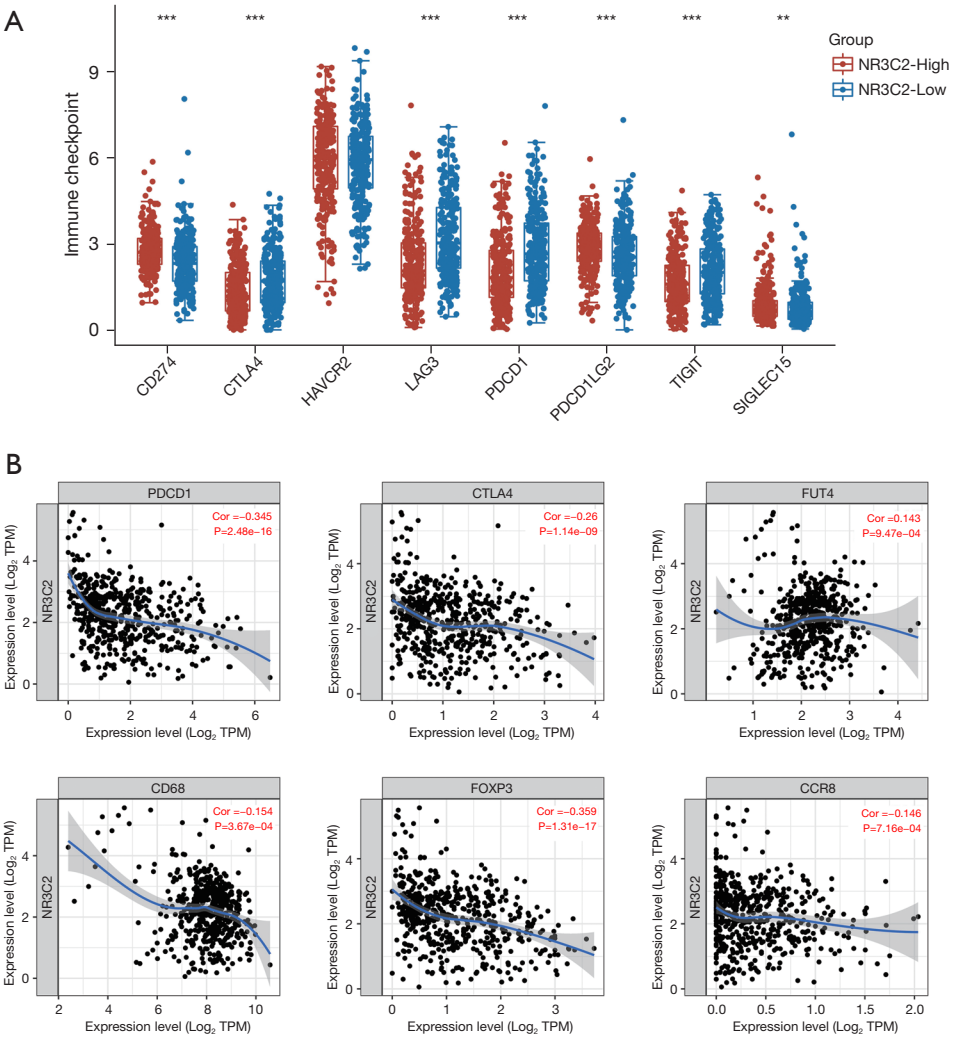

Figure 8 The association between *NR3C2* and immunosuppressive microenvironment in ccRCC. (A) A comparative analysis of eight immune checkpoints across various expression groups of *NR3C2*. (B) Correlation of *NR3C2* expression with markers of immunosuppressive cells. **, P<0.01; ***, P<0.001. ccRCC, clear cell renal cell carcinoma; TPM, transcripts per million.

NR3C2 expression. Additionally, we utilized a large-scale online database to analyze immune-related mechanisms for *NR3C2*. Based on the aforementioned results, we ultimately concluded that *NR3C2* may impede tumor progression by stimulating immune cell infiltration and hindering immune evasion.

TIICs are able to regulate the progression of cancer and may even have a prognostic value (17). A favorable prognosis has been linked to a high concentration of $CD8^+$ T cells that infiltrate tumors in the majority of cancer cases (18). And $CD4^+$ T cells can also mediate cytotoxicity in cancer (19). In RCC, the immune response is closely associated with the clinical outcome (20). Specifically, the study found that a heightened presence of $CD8^+$ T cells is linked to increased survival in chromophobe carcinoma, while an elevated level of quiescent memory $CD4^+$ T cells is associated with improved survival in ccRCC (21). Our study revealed that a high expression of *NR3C2* is indicative of a favorable prognosis in ccRCC patients, and *NR3C2* exhibited a significant positive correlation with both $CD8^+$ T cells and $CD4^+$ T cells. Based on the above information, it can be inferred that the favorable prognosis associated with high *NR3C2* expression in ccRCC is, in part, due to the augmented count of $CD8^+$ T cells or $CD4^+$ T cells.

The related mechanism of *NR3C2* has been reported. In ox-LDL-induced human coronary endothelial cells,

transcription of *NR3C2* promotes NLRP3 expression (22). The inhibition of proliferation and induction of cell cycle arrest in colorectal cancer cells was observed with *NR3C2* (23). In ccRCC cells, microRNA-155-5p overexpression or silencing had a significant impact on cell phenotype (24). In breast cancer cells, miR-301b-3p regulated the malignant phenotype through *NR3C2* (25). In addition, the gene *NR3C2* was identified as the target of miR-766 and was found to be involved in the β-catenin signaling pathway, resulting in the inhibition of proliferation and metastasis of liver cancer cells (26). *NR3C2* overexpression inhibited LoVo cell proliferation by inhibiting AKT/ERK signaling (27). In this study, we performed a preliminary study to investigate the relationship between *NR3C2* and TIM of ccRCC.

Immune checkpoints are critical molecules that regulate T-cell function (28). The exhaustion of T-cells is now considered a major factor in tumor progression (29). In addition, multiple immune checkpoints are expressed during T-cell exhaustion, including PD-1, CTLA-4, LAG-3, and T-cell immunoglobulin and ITIM domains (30). Immunotherapies that block immune checkpoints have revolutionized cancer treatment (31), and the magnitude of relevant research studies is substantial (32). There have been documented instances of complete remissions in cancer patients as a result of immunotherapy or immuno-oncology combinations (33). In patients with RCC, there has been an increasing focus on the assessment of quality of life within the context of clinical trials for medical treatment (34). It has been shown that ICB plus TKI (IO/TKI) has shown great performance on improving patients' survival (35). However, most patients do not experience durable clinical benefits (36,37). While Simonetti *et al.* have already reported RANKL efficacy in predicting the clinical advantage of ICB therapy in individuals with metastatic RCC (38), the identification of biomarkers that accurately forecast treatment response remains an unresolved requirement (39,40). We explored the correlation between *NR3C2* expression and immune checkpoints, which provided new ideas for immunotherapies, and it is anticipated that significant advancements will be achieved in this particular domain within the forthcoming five-year period.

Nevertheless, this study involved a small sample size and with heterogenous patients only, and the relationship between *NR3C2* and the infiltration of immune cells in the tumor microenvironment has not been confirmed through *in vitro* and animal experiments. Therefore, more samples are being collected, additional experiments are being prepared to elucidate this matter.

Conclusions

In conclusion, our study provided evidence supporting the *NR3C2* could serve as a novel biomarker for predicting survival in patients with ccRCC and the molecular mechanisms owe partly to immune cell infiltration.

Acknowledgments

We thank Dr. Anil Chuanhan from Ohio State University for helping polish the language and proofread our draft.
Funding: The study was supported by the Natural Science Foundation of Fujian Province, China (No. 2022J01122348), the Natural Science Foundation of Fujian Province, China (No. 2022 J01312324), the Health Commission of Fujian Province Young & Middle-Aged Medical Backbone Talents Project (No.2020GGA077), the Natural Science Foundation of Fujian Province (No. 2020J01126), the Sailing Fund of Fujian Medical University (No. 2018QH1164) and the Scientific Fund of Sanming Science and Technology Bureau (No. 2018-5-1(7)).

Footnote

Reporting Checklist: The authors have completed the TRIPOD reporting checklist. Available at https://tcr.amegroups.com/article/view/10.21037/tcr-23-846/rc

Data Sharing Statement: Available at https://tcr.amegroups.com/article/view/10.21037/tcr-23-846/dss

Peer Review File: Available at https://tcr.amegroups.com/article/view/10.21037/tcr-23-846/prf

Conflicts of Interest: All authors have completed the ICMJE uniform disclosure form (available at https://tcr.amegroups.com/article/view/10.21037/tcr-23-846/coif). The authors have no conflicts of interest to declare.

Ethical Statement: The authors are accountable for all aspects of the work in ensuring that questions related to the accuracy or integrity of any part of the work are appropriately investigated and resolved. The study was conducted in accordance with the Declaration of Helsinki (as

revised in 2013).

References

1. Capitanio U, Bensalah K, Bex A, et al. Epidemiology of Renal Cell Carcinoma. Eur Urol 2019;75:74-84.
2. Leibovich BC, Lohse CM, Crispen PL, et al. Histological subtype is an independent predictor of outcome for patients with renal cell carcinoma. J Urol 2010;183:1309-15.
3. Shen C, Beroukhim R, Schumacher SE, et al. Genetic and functional studies implicate HIF1α as a 14q kidney cancer suppressor gene. Cancer Discov 2011;1:222-35.
4. Riley RS, June CH, Langer R, et al. Delivery technologies for cancer immunotherapy. Nat Rev Drug Discov 2019;18:175-96.
5. Bi K, He MX, Bakouny Z, et al. Tumor and immune reprogramming during immunotherapy in advanced renal cell carcinoma. Cancer Cell 2021;39:649-661.e5.
6. Rini BI, Battle D, Figlin RA, et al. The society for immunotherapy of cancer consensus statement on immunotherapy for the treatment of advanced renal cell carcinoma (RCC). J Immunother Cancer 2019;7:354.
7. de Kloet ER, Van Acker SA, Sibug RM, et al. Brain mineralocorticoid receptors and centrally regulated functions. Kidney Int 2000;57:1329-36.
8. ter Heegde F, De Rijk RH, Vinkers CH. The brain mineralocorticoid receptor and stress resilience. Psychoneuroendocrinology 2015;52:92-110.
9. Haas JG, Weber J, Gonzalez O, et al. Antiviral activity of the mineralocorticoid receptor NR3C2 against Herpes simplex virus Type 1 (HSV-1) infection. Sci Rep 2018;8:15876.
10. Lu J, Hu F, Zhou Y. NR3C2-Related Transcriptome Profile and Clinical Outcome in Invasive Breast Carcinoma. Biomed Res Int 2021;2021:9025481.
11. Li X, Yang A, Wen P, et al. Nuclear receptor subfamily 3 group c member 2 (NR3C2) is downregulated due to hypermethylation and plays a tumor-suppressive role in colon cancer. Mol Cell Biochem 2022;477:2669-79.
12. Zhao Z, Zhang M, Duan X, et al. Low NR3C2 levels correlate with aggressive features and poor prognosis in non-distant metastatic clear-cell renal cell carcinoma. J Cell Physiol 2018;233:6825-38.
13. Barrett T, Wilhite SE, Ledoux P, et al. NCBI GEO: archive for functional genomics data sets--update. Nucleic Acids Res 2013;41:D991-5.
14. Sato Y, Yoshizato T, Shiraishi Y, et al. Integrated molecular analysis of clear-cell renal cell carcinoma. Nat Genet 2013;45:860-7.
15. Li T, Fan J, Wang B, et al. TIMER: A Web Server for Comprehensive Analysis of Tumor-Infiltrating Immune Cells. Cancer Res 2017;77:e108-10.
16. Zheng C, Zheng L, Yoo JK, et al. Landscape of Infiltrating T Cells in Liver Cancer Revealed by Single-Cell Sequencing. Cell 2017;169:1342-1356.e16.
17. Grivennikov SI, Greten FR, Karin M. Immunity, inflammation, and cancer. Cell 2010;140:883-99.
18. Fridman WH, Pagès F, Sautès-Fridman C, et al. The immune contexture in human tumours: impact on clinical outcome. Nat Rev Cancer 2012;12:298-306.
19. Oh DY, Fong L. Cytotoxic CD4(+) T cells in cancer: Expanding the immune effector toolbox. Immunity 2021;54:2701-11.
20. Díaz-Montero CM, Rini BI, Finke JH. The immunology of renal cell carcinoma. Nat Rev Nephrol 2020;16:721-35.
21. Zhang S, Zhang E, Long J, et al. Immune infiltration in renal cell carcinoma. Cancer Sci 2019;110:1564-72.
22. Chen X, Li W, Chang C. NR3C2 mediates oxidised low-density lipoprotein-induced human coronary endothelial cells dysfunction via modulation of NLRP3 inflammasome activation. Autoimmunity 2023;56:2189135.
23. Liu H, Lei W, Li Z, et al. NR3C2 inhibits the proliferation of colorectal cancer via regulating glucose metabolism and phosphorylating AMPK. J Cell Mol Med 2023;27:1069-82.
24. Yan C, Wang P, Zhao C, et al. MicroRNA-155-5p Targets NR3C2 to Promote Malignant Progression of Clear Cell Renal Cell Carcinoma. Kidney Blood Press Res 2022;47:354-62.
25. Fan Y, Li Y, Zhu Y, et al. miR-301b-3p Regulates Breast Cancer Cell Proliferation, Migration, and Invasion by Targeting NR3C2. J Oncol 2021;2021:8810517.
26. Yang C, Ma X, Guan G, et al. MicroRNA-766 promotes cancer progression by targeting NR3C2 in hepatocellular carcinoma. FASEB J 2019;33:1456-67.
27. Li J, Xu Z. NR3C2 suppresses the proliferation,

migration, invasion and angiogenesis of colon cancer cells by inhibiting the AKT/ERK signaling pathway. Mol Med Rep 2022;25:133.
28. Topalian SL, Taube JM, Anders RA, et al. Mechanism-driven biomarkers to guide immune checkpoint blockade in cancer therapy. Nat Rev Cancer 2016;16:275-87.
29. Wherry EJ, Kurachi M. Molecular and cellular insights into T cell exhaustion. Nat Rev Immunol 2015;15:486-99.
30. Blackburn SD, Shin H, Haining WN, et al. Coregulation of CD8+ T cell exhaustion by multiple inhibitory receptors during chronic viral infection. Nat Immunol 2009;10:29-37.
31. Finck AV, Blanchard T, Roselle CP, et al. Engineered cellular immunotherapies in cancer and beyond. Nat Med 2022;28:678-89.
32. Santoni M, Rizzo A, Mollica V, et al. The impact of gender on The efficacy of immune checkpoint inhibitors in cancer patients: The MOUSEION-01 study. Crit Rev Oncol Hematol 2022;170:103596.
33. Santoni M, Rizzo A, Kucharz J, et al. Complete remissions following immunotherapy or immuno-oncology combinations in cancer patients: the MOUSEION-03 meta-analysis. Cancer Immunol Immunother 2023;72:1365-79.
34. Rizzo A, Mollica V, Dall'Olio FG, et al. Quality of life assessment in renal cell carcinoma Phase II and III clinical trials published between 2010 and 2020: a systematic review. Future Oncol 2021;17:2671-81.
35. Wang J, Zhang S, Wang Y, et al. The prognostic significance of CDK6 expression in renal cell carcinoma treated by immune checkpoint plus tyrosine kinase inhibition. Scand J Immunol 2023;98:e13304.
36. Motzer RJ, Penkov K, Haanen J, et al. Avelumab plus Axitinib versus Sunitinib for Advanced Renal-Cell Carcinoma. N Engl J Med 2019;380:1103-15.
37. Motzer RJ, Tannir NM, McDermott DF, et al. Nivolumab plus Ipilimumab versus Sunitinib in Advanced Renal-Cell Carcinoma. N Engl J Med 2018;378:1277-90.
38. Simonetti S, Iuliani M, Stellato M, et al. Extensive plasma proteomic profiling revealed receptor activator of nuclear factor kappa-B ligand (RANKL) as emerging biomarker of nivolumab clinical benefit in patients with metastatic renal cell carcinoma. J Immunother Cancer 2022;10:e005136.
39. Fotia G, Stellato M, Guadalupi V, et al. Current Status of Predictive Biomarker Development in Metastatic Renal Cell Carcinoma. Curr Oncol Rep 2023;25:671-7.
40. Rosellini M, Marchetti A, Mollica V, et al. Prognostic and predictive biomarkers for immunotherapy in advanced renal cell carcinoma. Nat Rev Urol 2023;20:133-57.

Cite this article as: Chen D, Yin Z, Chen Y, Bai Y, You B, Sun Y, Wu Y. Validation of prognostic signature and exploring the immune-related mechanisms for *NR3C2* in clear cell renal cell carcinoma. Transl Cancer Res 2023;12(10):2518-2532. doi: 10.21037/tcr-23-846

